# Measurements of Rb trap-loss collision spectra

D. Hoffmann, P. Feng, and T. Walker

*Department of Physics, University of Wisconsin—Madison, Madison, Wisconsin 53706*

Received February 19, 1993; revised manuscript received November 29, 1993

We describe studies of excited-state/ground-state collisions between optically trapped Rb atoms. Collision rates are deduced from the transients observed as atoms are loaded into a vapor-cell optical trap. The rates are measured as a function of the frequency of the light used to excite the atom pairs. A comparison of the results for $^{85}$Rb and $^{87}$Rb shows that excited-state hyperfine interactions play a vital role in the dynamics of the collisions. In addition, the absolute rates are smaller than those expected from recent models.

*PACS numbers*: 32.80.Pj, 30.80.Ps, 34.50.Rk

## 1. INTRODUCTION

Over the past decade advances in laser trapping and cooling have made it possible to produce atomic vapors that are cooled to temperatures of 100 $\mu$K and below. The most successful trap to date, the Zeeman-tuned optical trap (ZOT), has been demonstrated with numbers of trapped atoms exceeding $10^{10}$,[1,2] densities approaching $10^{12}$ cm$^{-3}$,[2] and ensemble spin polarization.[3] In addition this trap can capture atoms directly from a vapor cell.[4] A number of experiments have measured rates for excited-state collisions between optically trapped atoms.[5–13] These collisions are of interest because of the long collision times for trapped atoms, which approach 1 $\mu$s, that result from the combination of low velocities and sensitivity to long-range interactions. The most striking consequence of the long collision times is that excited-state collisions should be drastically altered by effects of spontaneous emission.

Figure 1 illustrates a simple model, originated by Gallagher and Pritchard,[14] for excited-state/ground-state collisions between two optically trapped alkali atoms. As two atoms approach each other from distances of 100 nm or more they absorb photons from the laser that traps the atoms and spontaneously emit photons after traveling, on the average, approximately 3 nm. At a separation of 50 nm or so, the absorption of a photon puts the atoms on a strongly attractive excited-state potential curve that can accelerate them toward each other to a separation of 5 nm or less without spontaneously emitting a photon. At these relatively small distances the atoms can change fine-structure state or emit a photon that is strongly red shifted with respect to the laser photon that was originally absorbed. In either case the excess energy appears as kinetic energy, and this kinetic energy is sufficient to eject the atoms from the trap. Thus excited-state collisions between trapped atoms can be observed by measuring the rates at which atoms leave the trap.

In this paper we present a detailed description of the measurements of excited-state trap-loss collisions of Rb atoms that we have reported briefly in previous papers.[10,13] These measurements involve observations of the number of trapped atoms as a function of time as the atoms are captured by a vapor-cell ZOT[4] and emphasize the use of an additional laser[7] that is used to study the collision rates as a function of the laser frequency. This catalysis laser technique has the useful feature that it reveals information about the dynamic aspects of the collisions. Specifically, it gives information about the motion of the atoms at large interatomic separations before the atoms reach the energy-transfer region at small separations. This motion is affected by the excitation process, by acceleration on the excited-state potential(s), and by spontaneous emission. The primary result of our measurements is the unambiguous demonstration that excited-state hyperfine structure plays an important role in the collision dynamics. This demonstration consists of measuring the frequency dependence of the trap-loss collision rates (trap-loss spectrum) for the two common isotopes of Rb, $^{85}$Rb and $^{87}$Rb. For excitation of the atom pairs at frequencies within the excited-state hyperfine structure (region a in Fig. 2) a large isotopic difference is observed. At detunings of approximately one natural linewidth, this effect was previously observed by Wallace *et al.*[11] However, at detunings outside the excited-state hyperfine structure (region b in Fig. 2) the collision rates are the same for the two isotopes. We conclude that the hyperfine structure plays a vital role in these collisions.

This paper is organized as follows. In Section 2 we present the basic phenomenology of trap-loss collisions, outline our basic approach for investigating these collisions, summarize our results, and discuss their implications. In Section 3 we describe our trapping apparatus. In Section 4 we analyze how the collisions affect the operation of the trap and describe the catalysis laser technique for determining the trap-loss spectra. In Section 5 we show how we put the trap-loss spectra on an absolute scale.

## 2. TRAP-LOSS SPECTRA OF Rb

The Gallagher–Pritchard model[14] with refinements to include fine-structure[15] and nonperturbative effects of the laser fields,[16] has been the most successful model of trap-loss collisions to date. This model, illustrated in Fig. 1(a), separates the trap-loss rates into two factors. The first factor, which we refer to as

0740-3224/94/050712-09$06.00 

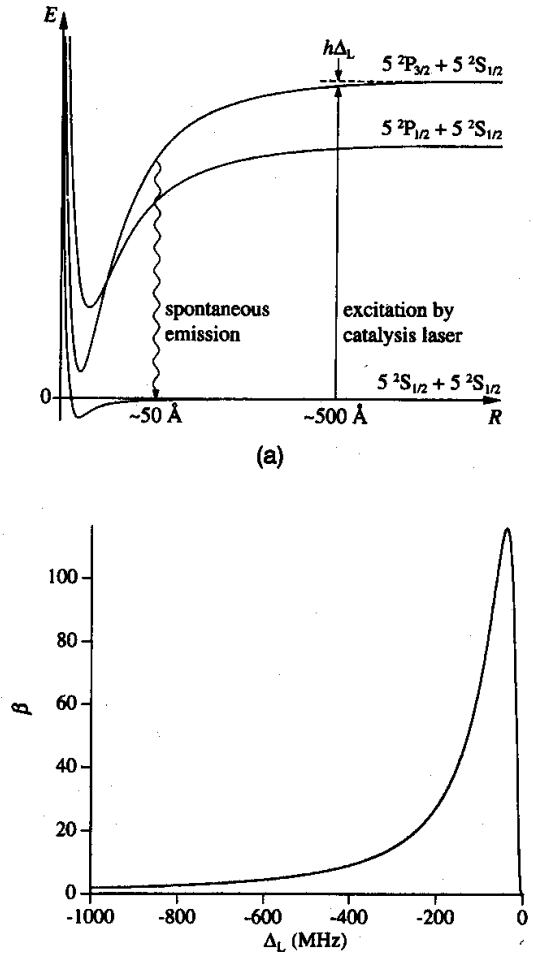


Fig. 1. Gallagher–Pritchard model for excited-state collisions of laser-cooled Rb atoms. (a) A colliding pair of atoms in the ground state absorb a photon from the laser to an attractive $R^{-3}$ excited-state potential curve. The atoms are accelerated along this curve toward each other. If the atoms do not spontaneously radiate to the ground state, thus terminating the excited-state collision, then at small internuclear separations they may either emit a red-shifted photon, as shown, or change fine-structure state. The resulting large amount of kinetic energy of the atoms causes them to leave the trap. (b) Characteristic trap-loss spectrum for Rb or Cs as predicted by this model.

a dynamic factor, is the rate at which atoms reach the small interatomic separation region at which energy transfer can occur. This arrival rate depends on the laser excitation rates, the amount of acceleration of the atoms caused by the excited-state potential curves (including, in principle, nonadiabatic effects of avoided crossings, although these are not yet in the models), and the spontaneous emission probability. The second factor that determines the trap-loss rate is the probability that energy transfer occurs once the atoms arrive at small interatomic separations. At this point the kinetic energy of the atoms is 1 K or more, which is sufficiently high that the physics that determines the energy-transfer probability is likely to be similar to higher-temperature collision experiments. However, because the atoms reach this region with very well-defined velocities, interference effects that are averaged out by the thermal motion at room temperature may be important in calculations of energy-transfer probabilities.[17]

The dynamic factor is most interesting because it involves radiative effects, in particular spontaneous emission during the collision, that are not present in high-temperature experiments. In the original Gallagher–Pritchard model the multiple excited-state potential curves are replaced by a single effective potential curve, and the trap-loss rate is given as

$$\beta n^2 \propto n^2 \int 4\pi R^2 \mathrm{d}R\, \mathcal{R}(R, \Delta_L) \exp[-t(R)/\tau]. \qquad (1)$$

Here $n4\pi R^2 \mathrm{d}R$ is the number of atom pairs at a distance $R$, $\mathcal{R}(R, \Delta_L)$ is the excitation rate of these pairs to the excited-state potential resulting from a laser whose frequency is detuned from the atomic resonance frequency by $\Delta_L$, $t(R)$ is the time required for atoms to reach small separation, and $\tau$ is the excited-state spontaneous emission time. Therefore $\exp[-t(R)/\tau]$ is the probability that the excited atom pair reaches small interatomic separation without radiating. The excited-state potential enters this equation in two places: it determines at which distances the excitation rate is resonant, and it determines the time required for the atoms to reach the energy-transfer region.

When the laser is detuned to the red of the atomic resonance line by an amount that is large compared with the natural width of the atomic line, and when motion arises from a single excited-state potential of the form $-C_3/R^3$, the trap-loss rate coefficient $\beta$ simplifies to

$$\beta \propto \left(\frac{\Delta_\tau}{\Delta_L}\right)^2 \exp[-(\Delta_\tau/\Delta_L)^{5/6}], \qquad (2)$$

with the characteristic shape shown in Fig. 1(b). $\Delta_\tau$ sets the frequency scale for the collisions and is given by

$$\Delta_\tau = \frac{C_3}{\hbar}\left(\frac{\mu}{3.59 C_3 \tau^2}\right)^{3/5} \approx 115\ \mathrm{MHz} \qquad (3)$$

for the heavy alkali metals Cs and Rb. Here $\mu$ is the reduced mass of the colliding atoms.

It is evident from the above considerations that a powerful technique for studying the dynamics of the collisions is to measure trap-loss spectra of the type modeled in

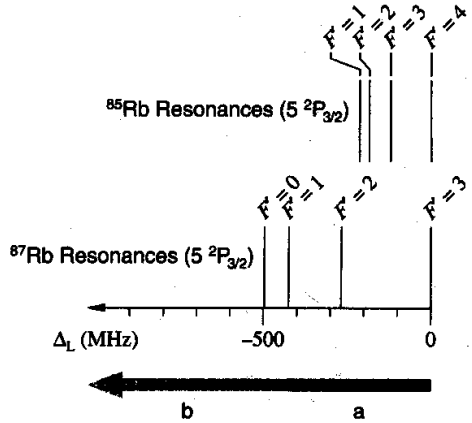


Fig. 2. Atomic excited-state hyperfine spectrum for $^{85}$Rb and $^{87}$Rb. In region a we observe a strong isotope effect in the collision spectra, and in region b the spectra are the same (see Fig. 4).

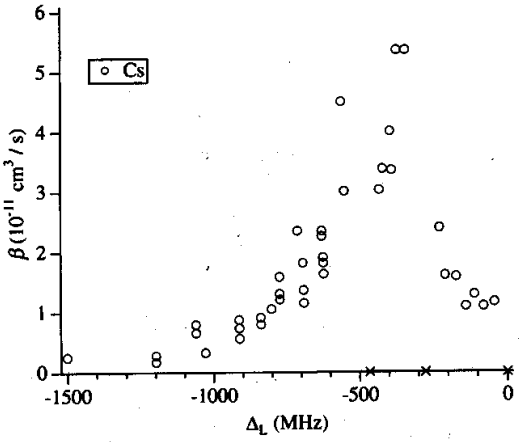


Fig. 3. Measured trap-loss spectrum for Cs from Ref. 8 for $I_c = 10\ \mathrm{mW/cm^2}$. The marks on the abscissa denote the positions of the atomic hyperfine resonances.

Fig. 1(b). Because the atoms cannot be trapped over the large range of laser frequencies shown in the figure, it is advantageous to add another laser, the catalysis laser, to the trap. The role of the catalysis laser is to enhance excited-state collision rates without affecting the operation of the trap. This technique was first used for Cs,[7,8] and the results are shown in Fig. 3. The general shape of the spectrum was found to be approximately as expected but broader than predicted and with the position of the maximum at larger detunings than expected. As shown, the spectrum peaks near the position of the lowest-frequency atomic hyperfine resonance. Still, it is not obvious from the Cs data alone whether the maximum arises at larger detunings as a result of $\Delta_\tau$ being incorrectly predicted by the Gallagher–Pritchard model or whether the neglect of features such as hyperfine structure is responsible.

In Fig. 4 we show our analogous measurements of the trap-loss spectra for the two stable isotopes of Rb, $^{85}$Rb and $^{87}$Rb, and include the small detuning measurements of Wallace *et al.*[11] We see that for $^{85}$Rb and $^{87}$Rb the maxima in the spectra occur at the position of the lowest-frequency component of the atomic hyperfine structure, just as for Cs. Furthermore, for $^{87}$Rb another maximum occurs near the next atomic hyperfine resonance, and for small detunings the rate coefficients for the two isotopes differ greatly. For large detunings no experimentally significant isotopic dependence is observed.

From these results we see that the excited-state hyperfine interaction has a profound effect on the trap-loss spectra. On the basis of the ideas behind the Gallagher–Pritchard model, there are several natural reasons why this effect occurs.[13] First, the modification of the potential curves by the hyperfine interaction will change the excitation function $\mathcal{R}(R, \Delta_L)$ in relation (2). For a given detuning there will generally be a number of different potential curves that can be resonantly excited by the catalysis laser. Second, the hyperfine interaction will affect the survival probability both through $t(R)$ and the spontaneous emission time $\tau$. Third, curve crossings and avoided crossings that arise from the interplay of the hyperfine interaction with the dipole–dipole interaction will affect the acceleration process once the atoms have been excited. To illustrate this effect, we show in Fig. 5 selected potential curves[18] for $^{87}$Rb. For the catalysis laser tuned as shown, successful acceleration of the atoms toward each other can happen only if a nonadiabatic transition occurs at the avoided crossing of the potentials. This could explain the observed isotopic difference for detunings within the excited-state hyperfine structure because it is within that detuning region that most of the avoided crossings will occur. For large detunings the $^{85}$Rb and $^{87}$Rb curves are similar, and so the isotopic difference is small.

An interesting feature of the $^{87}$Rb data (and possibly the Cs data) is the minimum in the region between the lower two atomic hyperfine resonances. This minimum is somewhat surprising as we might expect multiple peaks

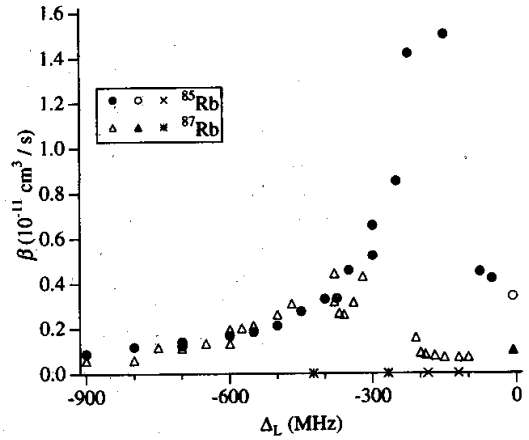


Fig. 4. Measured trap-loss spectra for $^{85}$Rb and $^{87}$Rb for $I_{\mathrm{ref}} = 10\ \mathrm{mW/cm^2}$. We have also included the two data points reported by Wallace *et al.*[11] at 5-MHz detuning. The marks on the abscissa denote the positions of the atomic hyperfine resonances. We obtained the data by changing the catalysis-laser intensity in order to hold the number of atoms constant as the catalysis-laser frequency is changed. The data are then scaled to $10\ \mathrm{mW/cm^2}$ by the assumption of a linear intensity dependence of the collisional rate coefficient $\beta$. The isotopic difference measured at small detunings, coupled with the lack thereof at large detunings, points to excited-state hyperfine structure as being the primary effect that has been left out of the collisional models to date.

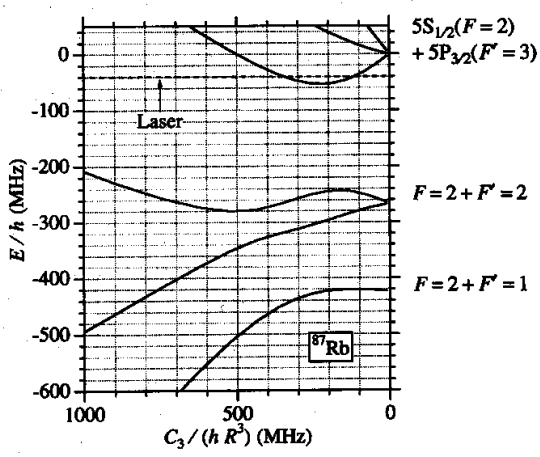


Fig. 5. Some of the excited-state potential curves relevant to trap-loss collisions of $^{87}$Rb atoms. Excitation of an atom pair at a catalysis-laser frequency as shown will not lead to trap loss unless nonadiabatic transitions occur to attractive potential curves. The value of $C_3$ for Rb is 0.071 eV nm$^3$.

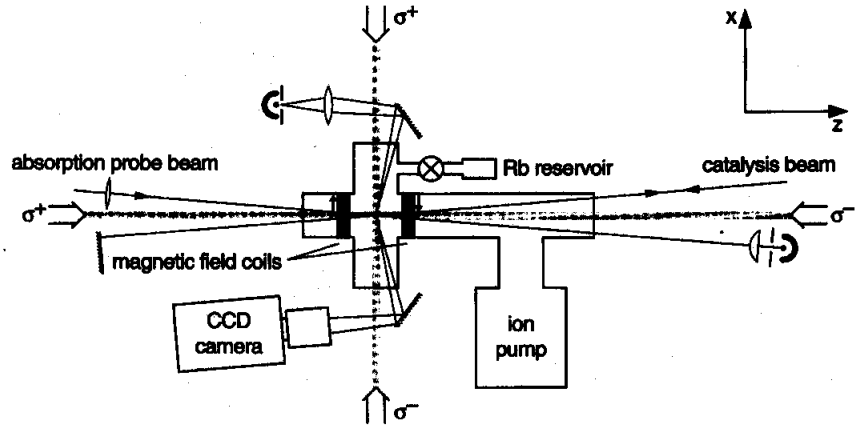


Fig. 6. Schematic of the apparatus.

to arise to the red side of the atomic resonances if the effect of hyperfine structure is simply to make the spectrum a sum of contributions similar to Fig. 1(b) but shifted by the atomic hyperfine splittings. In this case the minimum would be near the lower hyperfine resonance, in contrast to our results that find the minimum approximately halfway between the two atomic hyperfine resonances. We have no simple explanation for the position of the minimum but speculate that it may arise from modification of the excitation rates in the region of avoided crossings of the molecular potentials.[19]

So far we have concentrated on the shapes of the spectra, but the absolute rates are also of interest. Because the absolute rates depend on both the dynamic factors as well as the energy-transfer probabilities, a successful comparison of theory and experiment requires accurate calculations of both the dynamics and the energy-transfer probabilities. Despite the neglect of hyperfine effects on the dynamics by the models, there is quantitative agreement between theory and experiment for the case of Cs at small[15] and large[16] detunings. These calculations predict that Rb trap-loss collisions should occur at a rate approximately twice that of Cs collisions.[15] Thus, our observation of a factor of 5 or more smaller rate than expected at small detunings for Rb, confirmed by Wallace *et al.*,[11] suggests inaccuracies in the calculated energy-transfer probabilities. Further calculations have been made that indeed show a strong sensitivity to the precise knowledge of the potential curves,[17] owing to interference effects. It is unclear whether this sensitivity can explain some of the isotopic difference in the trap-loss rates at very small detunings.

## 3. APPARATUS

In this section we describe our apparatus, at the heart of which is a cell-loaded ZOT.[4] Figure 6 shows a diagram of the apparatus. The vacuum chamber was constructed from standard 1.5-in. (3.8-cm) stainless-steel UHV components, with viewports for optical access from six directions. An 8-L/s ion pump provided a base pressure of $\sim 10^{-10}$ Torr. A reservoir containing Rb metal was connected through a valve to the vacuum chamber. We obtained a base Rb vapor pressure of $\approx 10^{-9}$ Torr in the chamber by opening the valve, heating the reservoir until the vapor pressure in the chamber reached the desired value, and then closing the valve. With the valve closed the Rb vapor pressure would slowly decrease over a time scale of several weeks. A pair of magnetic-field coils wound in opposite directions produced a magnetic quadrupole field of typically $\partial_z B_z = 2\partial_z B_x = 2\partial_y B_y \approx$ 25 G/cm at the center of the vacuum chamber.

The lasers used for the experiment were diode lasers (Sharp LT024MD0) that were stabilized with optical feedback from a grating in a manner similar to that described in Ref. 20. Two lasers were used for the trapping and hyperfine pumping and were locked to Doppler-free resonances by the use of standard saturated absorption spectroscopy. The trapping laser was locked 5–10 MHz to the red of the $^{85}$Rb $5^2S_{1/2}(F = 3) \rightarrow 5^2P_{3/2}(F' = 4)$ or the $^{87}$Rb $5^2S_{1/2}(F = 2) \rightarrow 5^2P_{3/2}(F' = 3)$ resonance (natural linewidth, 5.9 MHz). The detuning of the trapping laser was determined to ±1 MHz by linear interpolation referenced to the line centers of the above resonances and the nearest crossover resonances. The output beam was sent through an optical isolator and a spatial filter/telescope to produce a 1.5-cm-diameter beam, which was then passed through a $\lambda/2$ plate, a polarizing beam splitter, and a nonpolarizing beam splitter, producing three beams that were used for trapping along the $\pm\hat{x}$, $\hat{y}$, and $\hat{z}$ directions. The $\lambda/2$ plate was adjusted to make the intensity of the $\pm\hat{z}$ beam one half that of the others, thus compensating for the stronger magnetic-field gradient along the $\hat{z}$ direction and giving a roughly isotropic confining force for the atoms. The three beams were aligned to intersect at the center of the vacuum chamber and were passed through $\lambda/4$ plates to give the appropriate circular polarizations, some of which are shown in Fig. 6, for producing the standard ZOT.[21] The total spatially averaged intensity of the trapping laser light at the position of the trapped atoms was 5.0 ± 0.5 mW/cm$^2$. The saturation intensity for Rb is 3.1 mW/cm$^2$, averaged over Zeeman levels.

The hyperfine pumping laser was locked to the $^{85}$Rb $5^2S_{1/2}(F = 2) \rightarrow 5^2P_{3/2}(F' = 3)$ or the $^{87}$Rb $5^2S_{1/2}(F = 1) \rightarrow 5^2P_{3/2}(F' = 2)$ resonance and served to counteract occasional optical pumping into the untrapped hyperfine state.[21] The 1.5-cm-diameter beam from this laser was combined with the trapping laser beam in one of the beam splitters and produced an average intensity of 1.8 mW/cm$^2$ at the position of the trapped atoms.

A CCD video camera was focused onto the cloud of trapped atoms in order to observe its shape. We could

adjust the position and shape of the cloud by slightly changing the alignments of the trapping beams as well as by adding a trimming magnetic field by the use of extra coils or a permanent magnet. In this way the shape of the cloud of atoms could be made to be nearly spherical, and the growth of the cloud as atoms were added was observed to be symmetric. For quantitative measurements of the spatial distribution of the atoms, a single horizontal line of the video output was selected for analysis.

The fluorescence from the trapped atoms was measured with a photodiode. For measurements of the density of the trapped atoms, a small fraction of the trapping laser was split off and focused through the cloud of atoms in order to probe the absorption. These measurements will be described further in Section 5.

The catalysis laser was tuned to a specified frequency near the $^{85}$Rb $5^2S_{1/2}(F = 3) \rightarrow 5^2P_{3/2}$ or the $^{87}$Rb $5^2S_{1/2}(F = 2) \rightarrow 5^2P_{3/2}$ resonances by the use of an optical spectrum analyzer (finesse ~ 150; free spectral range, 300 MHz) as a frequency reference. To correct for slow drifts in the spectrum analyzer, we simultaneously measured a small fraction of the trapping laser output as a stable reference frequency. The catalysis laser beam, after passing through an optical isolator and an electro-optic intensity modulator, progressed through a telescope to produce a beam with a diameter of 3.0 mm. The beam entered the cell at a slight angle relative to one of the trapping beams and overlapped the cloud of trapped atoms. We obtained optimum alignment of the catalysis laser through the trapped-atom cloud by tuning the catalysis laser near one of the atomic resonances to put a force on the trapped-atom cloud. Adjustments were made to the catalysis-laser beam alignment to maximize the displacement of the cloud. For the experiment, retroreflection of the catalysis laser reduced its mechanical influence on the trapped atoms.

## 4. BASIC METHOD: FREQUENCY DEPENDENCE

We base our collisional rate measurements on observations of the number of trapped atoms as a function of time as slow atoms from the background Rb vapor are captured by (that is, loaded into) the trap. By contrast, other research[6,7,11] has studied the time dependence as the atoms leave the trap with no loading. In a cell trap the loading cannot be turned off without also affecting other trapping parameters.

The rate equation that governs the number of atoms in the trap $N$ is[10]

$$\frac{dN}{dt} = L - \gamma N - \beta \int n^2(\mathbf{r};N)d^3r. \tag{4}$$

Here $L$ is the rate at which atoms are loaded into the trap from the background vapor and depends on factors such as the Rb vapor pressure, the intersection volume of the trapping lasers, the temperature of the cell, and most importantly, the intensity and detuning of the trapping lasers and the magnetic field gradient.[4] $\gamma N$ is the rate at which atoms are lost from the trap owing to collisions with (hot) untrapped Rb vapor and other vacuum contaminants. This factor is expected to be relatively insensitive to the trapping parameters, although our method makes no assumptions about this effect. The last term in Eq. (4) is the rate at which atoms leave the trap owing to collisions between the trapped atoms. It depends on the rate coefficient $\beta$ as well as the spatial average of the square of the trapped-atom density $n(\mathbf{r};N)$, which depends parametrically on $N$.

The collision rate in Eq. (4) depends on $n$, the total atom density, but not on the atomic excited-state fraction, as would be the case with high-temperature collision experiments, because spontaneous emission causes the de-excitation of the colliding atoms before they interact with the catalysis laser. For further discussion of this point, see Ref. 9.

Two primary collision processes are known to contribute to the last term in Eq. (4). In addition to the excited-state/ground-state collisions of interest for this research, there are ground-state/ground-state collisions as well. The ground-state collisions involve the change of the hyperfine state of the colliding atoms, releasing one half the ground-state hyperfine energy splitting to each atom. This energy corresponds to 0.15 K for $^{85}$Rb and 0.33 K for $^{87}$Rb. These values can be comparable to typical trap depths for small trap-laser detunings or low intensities.[11] Ground-state collisions should have no catalysis-laser intensity dependence.

In contrast, the excited-state collisions have the important signature that they are linear in the intensity of the laser that excites the atoms.[7] Thus the addition of the catalysis laser to the trap inherently selects only excited-state collisions. In this case the rate coefficient is $\beta = \beta_t + \beta_c$, where $\beta_t$ represents the rate coefficient with only the trapping lasers present (this may include contributions from both ground-state and excited-state collisions) and $\beta_c$ is the contribution of the catalysis laser.

If a linear intensity dependence for $\beta_c$ is assumed, the frequency dependence of the excited-state collisions (trap-loss spectrum) can be obtained directly from the steady-state behavior of Eq. (4). In the steady state we have

$$N = \frac{L}{\gamma + \beta\left(\int n^2(\mathbf{r};N)d^3r\right)\Big/N}. \tag{5}$$

Although changes in the catalysis-laser detuning $\Delta_c$ affect both $\beta$ and the atomic density distribution, we can adjust the intensity $I_c(\Delta_c)$ of the catalysis laser to hold the number of atoms constant as we vary $\Delta_c$, and the density distribution will remain constant as well. In this case

$$\beta = \beta_t + \beta_c(\Delta_c)I_c(\Delta_c)/I_{\text{ref}} \tag{6}$$

is independent of $\Delta_c$, so $\beta_c(\Delta_c)$ is inversely proportional to $I_c(\Delta_c)$. For our data presentation in Fig. 4, we then scale $\beta_c$ linearly by the assumption of a constant catalysis-laser intensity $I_{\text{ref}}$ of 10 mW/cm$^2$.

There is a significant advantage to adjusting the catalysis-laser intensity in order to hold the number of atoms in the trap constant. Because the density distribution is inherently difficult to measure, the separate density measurements at each catalysis-laser detuning that would otherwise be required would cause unnecessary scatter in the trap-loss spectra. By holding the

number of trapped atoms constant, the density distribution is also held fixed and therefore affects only the absolute scale and not the shape of the trap-loss spectrum. Thus, to the extent that the trapping lasers can be held stable over time, the determination of relative values of $\beta_c$ at various detunings is much more reliable than if the density distribution is measured separately for each detuning. For these reasons, the resulting collision spectra were found to be much more reproducible than measurements taken when $N$ was not held constant. On the basis of the reproducibility of the shapes of the spectra, we estimate the relative error of the measurements at different frequencies to be ~20%.

The reliability of this method depends on the assumption that the catalysis laser affects only the collisions and in particular does not affect the density distribution of the atoms. This assumption is most likely to be violated when the catalysis laser is tuned near one of the atomic hyperfine resonances. We performed a number of tests to verify that the catalysis laser did not affect the trapped atoms for this experiment (aside from trap-loss collisions). When any of these tests failed, the data were discarded. First, with the video camera we monitored the position of the cloud to make sure it did not change when the catalysis laser was blocked or unblocked. Second, we monitored the fluorescence from the trapped atoms as the catalysis laser was blocked or unblocked. If a rapid (millisecond) change in the fluorescence was observed, this was taken as evidence that the catalysis laser was causing significant (and unwanted) optical pumping of the atoms. This effect could sometimes be observed even though no motion of the cloud of atoms was evident. Third, using the video signal from the camera, we monitored the distribution of the atoms in the trap. Sometimes the distribution of the trapped atoms fluctuated visibly owing to the catalysis laser even though the overall position of the cloud did not change. Finally, because it is conceivable that the catalysis laser might affect the loading rate without affecting the trapped atoms, we checked for possible variations in the loading rate by studying the rate at which atoms were captured into an initially empty trap with and without the catalysis laser in the trap. Because the solution of Eq. (4) at small $t$ is $N(t) = Lt$, the slope of the number of atoms versus time does not depend on the presence of the catalysis laser unless the catalysis laser is affecting $L$.

Although the role of the catalysis laser is to cause collisions without affecting the trapped atoms, it is possible that the catalysis-laser-produced collision rates are affected by the presence of the trapping light. This effect might arise, for example, by the trapping laser affecting the flux of colliding atoms, by optical pumping, or by ac Stark shifts. We expect that the optical pumping and flux-changing effects will principally affect the magnitudes of the measured rates and not the shapes of the spectra because the trapping lasers interact with the atoms at larger interatomic separations than does the catalysis laser. Therefore, these effects should be independent of the catalysis-laser detuning. The ac Stark shifts are only a few megahertz and so should not have any marked effect on the much broader features studied here. We do not believe that any of the above effects are important for the data that we present, as evidenced by the reproducibility of our absolute rate measurements at the 30% level when the trapping laser intensity and frequency are changed (see Section 5).

The measured trap-loss spectra are shown in Fig. 4, and their significance is discussed in Section 2. In Fig. 4 we have placed the measurements on an absolute scale, which requires a more detailed study of $N$ versus $t$, as described in Section 5.

## 5. ABSOLUTE CALIBRATION

In this section we discuss the determination of an absolute scale for the measured rate coefficients. We do this by measuring loading transients that obey Eq. (4). Here, a critical issue is the inherent nonlinearity of the term $\beta \int n^2(\mathbf{r};N)\mathrm{d}^3r$ that represents the collisions between the trapped atoms. In particular, a complication arises because of radiation trapping, which forces the density distribution $n(\mathbf{r};N)$ to depend in general on the number of atoms in the trap. This complication is why other experiments[6,7,11] have worked with small numbers of atoms, typically $N < 10^4$, where the absence of radiation trapping effects means that the shape of the distribution is independent of the number of atoms in the trap and hence independent of time as the atoms are ejected from the trap owing to collisions. However in our experiment, with the number of trapped atoms in the cloud exceeding $10^6$, radiation trapping[22,23] causes the cloud to expand, thus changing the shape of $n(\mathbf{r})$. To extract the collision rates by observing the number of atoms versus time, we need to understand how the density distribution changes with time or, equivalently, how the density distribution depends on $N$. We will show that for $N \gtrsim 10^6$, a good approximation is to consider the density distribution to be approximately spatially uniform, with a correction to account for the smooth reduction of the density from its maximum value to zero near the outer edge of the trapped-atom cloud.

We base our analysis on the radiation trapping model of Sesko *et al.*[23] When the number of atoms in an optical trap is small, the atoms move independently of each other and the spatial distribution of the atoms is determined by the shape of the trapping force field and the temperature. For a force proportional to displacement, $\mathbf{F} = -k\mathbf{r}$, the distribution is $n(\mathbf{r}) = n(0)\exp(-kr^2/2T)$, where $T$ is the temperature and $\mathbf{F}$ and $k$ are expressed in terms of temperature units. When the number of atoms confined by the trap is very large, the density distribution is dominated by radiation trapping and is given by

$$n(\mathbf{r}) = \begin{cases} n_{\max} & r < \left(\dfrac{3N}{4\pi n_{\max}}\right)^{1/3} \\ 0 & \text{otherwise} \end{cases}. \tag{7}$$

In general, neither limiting case is appropriate, and it is necessary to consider the intermediate regime in which both nonzero temperature and radiation trapping are important. Figure 7 shows density distributions in the intermediate regime. A convenient parameter for discussing this case is $N_{rt} \equiv 4\pi n_{\max}(T/k)^{3/2}$, which is nearly the number of atoms contained in a uniform sphere of radius $(2T/k)^{1/2}$. As shown in Fig. 7, for $N/N_{rt} = 0.10$ or

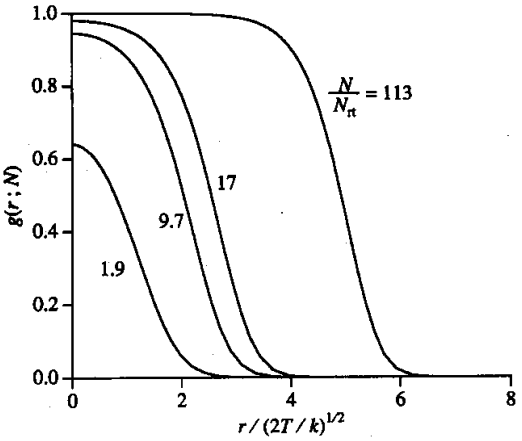


Fig. 7. Theoretical density distributions of optically trapped atom clouds for nonzero temperatures at various numbers of trapped atoms. $n_{max}$ is the radiation trapping limited density, $T$ is the temperature of the atom cloud, and $k$ is the spring constant of the Zeeman trapping force; $(2T/k)^{1/2}$ is roughly the radius of the atom distribution when radiation trapping is not present. The number of atoms in the trap required for radiation trapping to begin to affect the atomic density distribution is approximately $N_{rt} = 4\pi n_{max}(T/k)^{3/2}$.

more the density is limited to the value $n_{max}$, so we can write $n(\mathbf{r};N) = n_{max}g(r;N)$ with $g(0;N) = 1$. A typical value for $n_{max}$ is $2 \times 10^{10}$ cm$^{-3}$, and $(2T/k)^{1/2}$ is typically approximately 150 $\mu$m, giving $N_{rt} = 3 \times 10^5$. For our experiment $N/N_{rt}$ is typically 20.

Although the density of the atoms is limited by radiation trapping to the value $n_{max}$, we need to consider the effect of temperature on the density distribution near the edge of the cloud. This effect is important because the collision rate $\beta \int n^2(\mathbf{r};N)\mathrm{d}^3r$ preferentially weights large $r$, where the nonzero temperature reduces the density below $n_{max}$. To include this effect, we rewrite Eq. (4) as

$$\frac{\mathrm{d}N}{\mathrm{d}t} = L - \gamma N - \beta n_{max}\left(\frac{\int g^2(r;N)\mathrm{d}^3r}{\int g(r;N)\mathrm{d}^3r}\right)N. \tag{8}$$

The factor in parenthesis,

$$f(N) \equiv \frac{\int g^2(r;N)\mathrm{d}^3r}{\int g(r;N)\mathrm{d}^3r}, \tag{9}$$

is a measure of the reduction of the collision rate owing to the nonuniform density distribution that arises from nonzero temperature. For $T = 0$, $f = 1$.

In Fig. 8 we present model calculations of $f(N)$ for various values of $N/N_{rt}$. The dependence of $f$ on $N$ is very weak, slower than logarithmic, approaching one only for $N/N_{rt} \gg 1000$. Because the dependence is so weak, we can approximate $f[N(t)]$ as being independent of time and rewrite Eq. (8) as

$$\frac{\mathrm{d}N}{\mathrm{d}t} = L - [\gamma + \beta n_{max}f(N_\infty)]N, \tag{10}$$

where $N_\infty = L/\Gamma$ and $\Gamma = \gamma + \beta n_{max}f(N_\infty)$. This equation has transient solutions

$$N(t) = N_\infty[1 - \exp(-\Gamma t)] \tag{11}$$

for when the initial condition is taken to be $N(0) = 0$. As Fig. 9 shows, Eq. (11) indeed fits the observed time dependence. Because $\gamma$ and $\beta n_{max}f(N_\infty)$ are not independently determined by a fit to Eq. (11), we use the catalysis-laser technique to isolate the contribution of $\beta$. To do this we collect two transients, one with the catalysis laser and one without, and the catalysis-laser contribution $\beta_c n_{max}f(N_\infty)$ is the difference between the two measured values of $\Gamma$.

The approximation $f(N) = f(N_\infty)$ is even better than suggested by Fig. 8 for two reasons. First, for small $t$ the transients depend only on the loading rate, $N = Lt$, so the collision rate does not affect the transients at small $t$. Second, the curvature of the transients, which determines $\Gamma$, is determined mainly by $0.5L/\Gamma < N < L/\Gamma$, and in this regime $f$ varies by at most 10%. As an additional test of this approximation, we have also measured

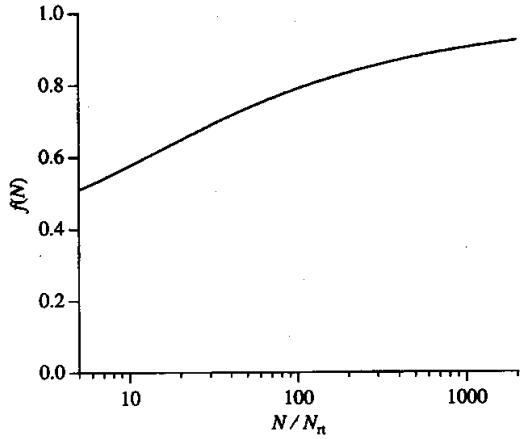


Fig. 8. Plot of the parameter $f(N)$, which measures the decrease of the binary collision rate for an optically thick cloud at finite temperature from the rate for zero temperature. The number of atoms in the trap required for radiation trapping to begin to affect the atomic density distribution is approximately $N_{rt} = 4\pi n_{max}(T/k)^{3/2}$.

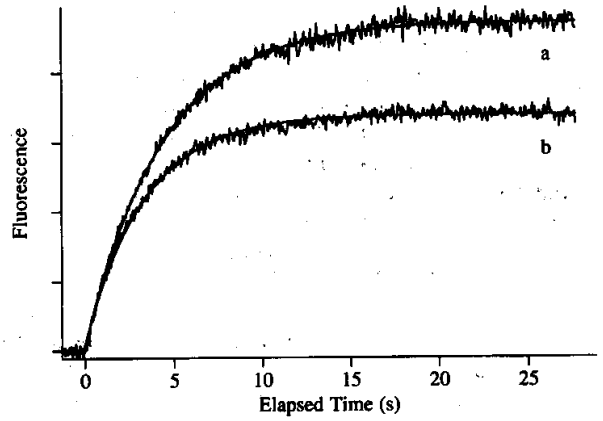


Fig. 9. Fluorescence from the cloud of trapped atoms during continual loading of atoms into the trap, with fits that use Eq. (11). Trace a is the observed transient with no catalysis laser present, and trace b shows the change produced by the addition of the catalysis laser.

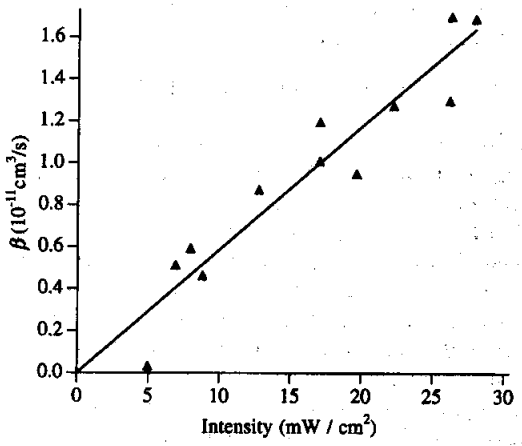


Fig. 10. Catalysis-laser intensity dependence for $^{85}$Rb at a detuning of −300 MHz.

transients for which the trap was allowed to fill without the catalysis laser present, then the catalysis laser was added, and the resulting transient was observed. The time constants measured in this way agreed to within better than 10% than those obtained in the manner described above. Alternatively, we can consider the fit of the exponential function in Eq. (11) as a convenient approximation that obeys the rigorous limits $N = Lt$ for small $t$ and $N = L/\Gamma = L/[\gamma + \beta n_{\max} f(N_\infty)]$ for large $t$.

To determine $\beta$ from the value of $\beta n_{\max} f(N_\infty)$ as deduced from the transients, we need an absolute measurement of the density distribution $n(\mathbf{r})$. The distribution is deduced from the CCD camera output, with an absolute scale set by an absorption measurement. In analyzing the data we have found a convenient parameterization for the density distribution to be

$$n(\mathbf{r}) = \frac{n_{\max}}{1 + \exp[(r - r_c)/r_T]}, \tag{12}$$

where $r_c$ is the radius at which the density falls to half its maximum value, and $r_T$ corresponds to the range of distances over which the density deviates from $n_{\max}$. This functional form fits the calculated distributions of Fig. 7 and the observed distributions quite well.

The procedure to determine $n(r)$ was to first determine $r_c$ and $r_T$ by a fit of the output of the CCD camera to the integral of Eq. (12) along the line of sight. Then we used the absorption measurement with a calculated absorption cross section to determine $n_{\max}$. Typical measured densities were in the range of $1 \times 10^{10}$ to $3 \times 10^{10}$ cm$^{-3}$. Using the distribution, we calculated $f(N_\infty)$ from Eq. (9). We checked this procedure for internal consistency by taking data at various trap-laser detunings and intensities and background Rb vapor pressures. The variation in our results was found to be ±30%, and the results were reproducible over several months.

Because the absorption measurement is performed with the trap on, a possible concern is the effect of Raman wave-mixing processes[24,25] on the absorption signals. These effects are prominent when the probe-laser and trapping-laser frequencies differ by ~1 MHz. However, because our probe used for absorption is split off from the trapping laser, it has precisely the same frequency, and so we do not expect the Raman processes to be important. To check, we also measured the density by using fluorescence (which is insensitive to these effects), and the results agreed to within 50%, the estimated uncertainty of the fluorescence measurement.

The measurement of the frequency dependence (Section 4) assumed a linear dependence of $\beta$ on the catalysis-laser intensity. The assumed linearity was checked in two ways. First, the trap-loss rate was measured from transients as described above at several catalysis-laser intensities for a single detuning of −300 MHz for $^{85}$Rb, as shown in Fig. 10. Second, the spectra were measured by the use of different catalysis-laser intensities, and the shape was found to be the same within experimental scatter. Because the method for obtaining the spectra relies on a linear intensity dependence, finding that the shapes of the spectra are independent of intensity is equivalent to doing an intensity dependence over the whole range of detunings.

## 6. CONCLUSIONS

We have measured trap-loss spectra for $^{85}$Rb and $^{87}$Rb atoms. The spectra reveal information concerning the dynamics of the trap-loss collisions that cannot be obtained by a simple measurement of the trap-loss rate due to the trapping lasers. In particular we have demonstrated the strong effects that the excited-state hyperfine interaction has on the collision dynamics. The catalysis-laser technique used here should be applicable to a wide variety of other excited-state collision processes. In particular experiments on associative ionization (for Na) or energy pooling would benefit from using two catalysis lasers.[26]

## ACKNOWLEDGMENTS

We thank J. D. Tobiason for a critical reading of the manuscript. We acknowledge the support of the University of Wisconsin Research Committee, National Science Foundation grants PHY-9213666 and PHY-9257058, and the Packard Foundation. T. Walker is an Alfred P. Sloan Research Fellow.

## REFERENCES

1. K. Gibble, S. Kasapi, and S. Chu, Opt. Lett. **17**, 526 (1992).
2. W. Ketterle, K. Davis, M. Joffe, A. Martin, and D. Pritchard, Phys. Rev. Lett. 70, 2253 (1993).
3. T. Walker, P. Feng, D. Hoffmann, and R. Williamson, Phys. Rev. Lett. **69**, 2168 (1992).
4. C. Monroe, W. Swann, H. Robinson, and C. Wieman, Phys. Rev. Lett. **65**, 1571 (1990).
5. P. Gould, P. Lett, P. Julienne, W. Phillips, H. Thorsheim, and J. Weiner, Phys. Rev. Lett. **60**, 788 (1988).
6. M. Prentiss, A. Cable, J. Bjorkholm, S. Chu, E. Raab, and D. Pritchard, Opt. Lett. **13**, 452 (1988).
7. D. Sesko, T. Walker, C. Monroe, A. Gallagher, and C. Wieman, Phys. Rev. Lett. **63**, 961 (1989).
8. T. Walker, D. Sesko, C. Monroe, and C. Wieman, "Collisional loss mechanisms in light-force atom traps," in *The Physics of Electronic and Atomic Collisions, XVI International Conference*, A. Dalgarno, R. Freund, P. Koch, M. Lubell, and T. Lucatorto, eds. (American Institute of Physics, New York, 1989), pp. 593–598.
9. P. Lett, P. Jessen, W. Phillips, S. Rolston, C. Westbrook, and P. Gould, Phys. Rev. Lett. **67**, 2139 (1991).

10. D. Hoffmann, P. Feng, R. Willamson, and T. Walker, Phys. Rev. Lett. **69,** 753 (1992).
11. C. Wallace, T. Dinneen, K. Tan, and P. Gould, Phys. Rev. Lett. **69,** 897 (1992).
12. F. Bardou, O. Emile, J. Courty, C. Westbrook, and A. Aspect, Europhys. Lett. **20,** 681 (1992).
13. P. Feng, D. Hoffmann, and T. Walker, Phys. Rev. A **47,** R3495 (1993).
14. A. Gallagher and D. Pritchard, Phys. Rev. Lett. **63,** 957 (1989).
15. P. Julienne and J. Vigue, Phys. Rev. A **44,** 4464 (1991).
16. Y. Band and P. Julienne, Phys. Rev. A **46,** 330 (1992).
17. O. Dulieu, J. Weiner, and P. Julienne, Phys. Rev. A **49,** 607 (1994).
18. T. Walker and D. Pritchard, "Effects of hyperfine structure on alkali trap-loss collisions," Laser Phys. (to be published).
19. M. O'Callaghan, A. Gallagher, and T. Holstein, Phys. Rev. A **32,** 2754 (1985).
20. C. Wieman and L. Holloberg, Rev. Sci. Instrum. **62,** 1 (1991).
21. E. Raab, M. Prentiss, A. Cable, S. Chu, and D. Pritchard, Phys. Rev. Lett. **59,** 2681 (1987).
22. T. Walker, D. Sesko, and C. Wieman, Phys. Rev. Lett. **64,** 408 (1990).
23. D. Sesko, T. Walker, and C. Wieman, J. Opt. Soc. Am. B **8,** 946 (1991).
24. J. Tabosa, G. Chen, Z. Hu, R. Lee, and H. Kimble, Phys. Rev. Lett. **66,** 3245 (1991).
25. D. Grison, B. Lounis, C. Salomon, J. Courtois, and G. Grynberg, Europhys. Lett. **15,** 149 (1991).
26. A. Gallagher, Phys. Rev. A **44,** 4249 (1991).